Astron. Astrophys. 214, 239–248 (1989)

ASTRONOMY AND ASTROPHYSICS

Oxygen in old and thick disk stars*

B. Barbuy [1,2] **and M. Erdelyi-Mendes** [1]

[1] Universidade de Sao Paulo, Depto. de Astronomia, C.P. 30627, Sao Paulo 01051, Brazil
[2] Observatoire de Paris, Section de Meudon, F-92195 Meudon Cedex, France

Received May 25, accepted September 5, 1988

Summary. High resolution Reticon and CCD spectra comprehending the |O I| λ6300.311 line were obtained for old and thick disk stars. The space velocities were studied in order to classify the stars in the different population groups. The atmospheric parameters were examined to be as accurate as possible and used to determine the oxygen abundance with synthetic spectrum calculations. The present results show that (a) oxygen seems to be overabundant relative to iron for metallicities [Fe/H] = −0.8; (b) for metallicities in the range $-0.8 < [Fe/H] < -0.5$, there seems to be a spread in the [O/Fe] ratios. This spread could be an indication of a thick disk phase in the chemico-dynamical evolution of the Galaxy. The scatter is however within the error bars of the determinations. Finally, it must be pointed out that a difference seems to appear between oxygen-to-iron ratios derived from the forbidden and the permitted lines.

Key words: oxygen abundances – synthetic spectra – stellar populations

1. Introduction

The stellar populations in the Galaxy can be subdivided in 3 groups, according to their chemical and kinematical properties: the extreme spheroid, the thick disk and the thin disk (Gilmore and Reid, 1983).

Oxygen-to-iron ratios in halo stars show a typical value [O/Fe] = 0.4 (Barbuy, 1988). At metallicities around $-1.2 < [Fe/H] < -0.6$, the oxygen-to-iron ratio decreases from 0.4 dex to reach the solar value for the more metal-rich stars. The precise metallicity at which the transition occurs could give an indication on the duration of the formation of the extreme spheroid, according to Gilmore and Wyse (1986).

The |O I| λ6300.311 line was observed in old disk stars in order to obtain an indication on the behaviour of the oxygen-to-iron ratio at the moderate metallicities $-1.3 < [Fe/H] < -0.4$.

The present sample contains stars with kinematic properties of the old disk, which makes this study somewhat different from those of Kjaergaard et al. (1982), Clegg et al. (1981), Nissen et al. (1985), Gratton and Ortolani (1986), devoted to the same problem, but where the samples were constituted mostly of typical disk stars.

High velocity and intermediate metallicity stars were selected from the catalogue of population II stars by Carney (1980). One very probably thick disk star from the list by Norris (1986) was also observed.

In Sect. 2 the observations are described, in Sect. 3 the space velocities are given, in Sect. 4 the atmospheric parameters are established, in Sect. 5 the oxygen abundances are derived, in Sect. 6 the results are discussed and in Sect. 7 conclusions are presented.

2. Observations

The spectra were obtained at the 1.4 m Coudé Auxiliary Telescope (CAT) telescope at the European Southern Observatory (ESO) at La Silla, Chile. The Coudé Echelle Spectrometer (CES) and a Reticon were used at a resolution of $R = 80000$ (or $\Delta\lambda = 0.08$ Å). In a few cases a short camera and a CCD (RCA with 640×1024 pixels of $15 \times 15\,\mu m^2$) at a resolution $R = 50000$ (or $\Delta\lambda = 0.13$ Å) were used. The exposures were made long enough for obtaining spectra with a high S/N ratio of the order of 200.

The reductions were done with the aid of the IHAP system available at the computers HP 1000 at ESO. For the CCD spectra the flatfield correction was done by dividing the spectrum of the program star by the spectrum of a featureless B star observed in the same conditions of observations; this procedure presents the advantages of correcting better for the flatfield and also of eliminating the telluric lines.

3. Program stars

The list of observed stars is shown in Table 1, where the visual magnitude, estimated absolute magnitude, distance modulus and distance, as well as space velocities including the radial velocities and velocities U, V, W in galactic coordinates, and the eccentricity are presented.

The absolute magnitudes for the stars of the present sample have been initially taken from Hansen and Kjaergaard (1971), Eggen (1979) and Norris et al. (1985). The values given in these references were checked and those for the remaining stars were established using the method of Sandage (1970): the $(B-V)$ colour is used to interpolate or extrapolate the absolute magnitude M_v, using the M_v versus $(B-V)$ diagram of a cluster of metallicity close to the star in question; colour-magnitude diagrams computed by VandenBerg and Bell (1985) were employed.

The space velocities U in the direction away from the galactic center, V in the direction of galactic rotation and W in the

Send offprint requests to: B. Barbuy (Brazilian address)

* Based on observations collected at the European Southern Observatory, La Silla, Chile

Table 1. Apparent magnitude, absolute magnitude and corresponding references, distance modulus, distance, radial velocity, velocities in galactic coordinates and eccentricity for the program stars

HD No.	V	M_V	Ref	$m-M$	R(pc)	RV	U	V	W	e
						km s^{-1}				
4308	6.54	4.7	1	1.84	23	100	−62	−110	−29	0.46
5268	6.16	2.25	5	3.91	60	44	4	− 1	−46	0.07
6254	8.01	2.0	5	6.0	160	53	27	− 68	−52	0.25
6734	6.46	2.7	2	3.76	56	−95	− 51	−137	32	0.55
7595	9.72	0.4	5	9.3	720	−44	− 82	− 30	40	0.29
10700	3.5	2.9	5	0.6	13	−16	− 52	+105	6	0.76
20619	7.04	3.0	5	4.04	64	20	39	− 76	15	0.29
37828	6.87	0.6	5	6.27	180	193	119	−167	−34	0.68
71597	7.31	0.0	1	7.31	290	110	61	−109	− 5	0.44
77236	7.54	0.0	1	7.54	322	142	−240	− 12	123	0.79
107328	4.96	0.5	5	4.46	78	36	30	− 77	− 3	0.29
119971	5.45	−1.0	1	6.45	195	20	−117	− 23	−66	0.40
130694	4.42	−1.0	4	5.41	120	−10	49	− 69	3	0.27
130952	4.94	1.5	2	3.44	49	83	− 65	− 73	− 5	0.34
136352	5.65	3.5	5	2.15	27	−69	119	− 82	66	0.43
175329	5.14	−1.2	1	6.34	185	180	−254	−161	−65	0.83
180928	6.06	0.5	5	5.56	130	−18	− 47	−166	−18	0.65
189567	6.07	3.9	5	2.17	27	−12	72	− 64	−24	0.29
203608	4.22	4.0	5	0.22	11	−30	11	50	6	0.36
206642	6.30	0.8	5	5.5	126	−58	53	−102	21	0.41
208998	7.13	3.45	1	3.68	54	−20	20	−120	41	0.46
211998	5.29	3.0	1	2.29	29	20	154	−125	−64	0.60
214690	5.87	0.3	5	5.57	130	79	−74	−108	−74	0.46
219615	3.69	1.4	2	2.29	29	−14	92	− 41	−24	0.28

References: (1) Eggen (1979), (2) Hansen, Kjaergaard (1971), (3) Norris et al. (1985), (4) Norris (1986), (5) see text.

direction towards the north galactic pole, as well as the eccentricity e were computed using formulae by Eggen et al. (1962), Eggen (1966). The proper motions and radial velocities were adopted from the archives of the Centre de Données Stellaires at Strasbourg (CDSS), from the catalogue of Population II field stars by Carney (1980) or from Norris (1986). The main uncertainties in the quantities derived in Table 1 come from the value of the absolute magnitude (or distance modulus or distance).

4. Atmospheric parameters

The accuracy of absolute abundances depends on the accuracy in the stellar parameters. Contrarily to the case of the determination of isotopic ratios, where a small error in the atmospheric parameters affects very little the results (e.g., Barbuy, 1985a), in the case of elemental abundances, the accuracy in the atmospheric parameters is crucial for the validity of the results. Therefore, atmospheric parameters for stars in common with Barbuy (1985a) are examined here with a greater care, being sometimes different from those given in that list.

Preliminary determinations for some stars of the present sample, were given in Barbuy (1985b), based on analyses from the literature.

In order to minimize the errors in the oxygen abundances, a reanalysis of each star has been done, and the data given in the literature are checked and adjusted as described below.

4.1. Interstellar extinction and temperatures

A mean extinction law as given by Bond (1980) has been used to compute the unreddened indices. The distances adopted follow those described in Sect. 3 and given in Table 1.

The temperature has been derived from the following photometric indices corrected for extinction: $(B-V)$, Strömgren $(b-y)$, Geneva (B2–V1), Johnson's $(R-I)$, $(V-R)$ and $(V-K)$, where relations with the temperature are given by Carbon et al. (1987) for $(B-V)$, Carney (1983) for $(b-y)$, $(R-I)$, $(V-K)$, Golay (1980) for (B2–V1) and Stone (1983) for $(V-R)$. The photometric data and derived temperatures are given in Table 2. The sources of data are: the Strömgren photometry is given by Lindgren and Ardeberg (in a catalogue in preparation); the Geneva index (B2–V1) is given by Rufener (1981); the other indices were found in Carney (1980) and at the CDSS.

A check of the temperature is further done by deriving from the spectra the temperature satisfying the excitation equilibrium, using curves of growth of Fe I, the only species presenting a sufficient number of lines available.

4.2. The metallicity

4.2.1. The oscillator strengths gf's

The gf's were obtained, for all lines in the region $\lambda\lambda$ 6285–6333, by fitting synthetic spectra to the solar spectrum (Delbouille et al.,

Table 2. Apparent magnitude, colour indices $(B-V)$, Strömgren $(b-y)$, m_1, c_1, Geneva $(B2-V1)$, Johnson $(R-I)$, $(V-R)$, $(V-K)$, interstellar extincition $E(B-V)$, and derived corresponding reciprocal temperatures

HD No.	V	$(B-V)$	$(b-y)$	m_1	c_1	$(B2-V1)$	$(R-I)$	$(V-R)$	$(V-K)$	$E(B-V)$	$\theta(B-V)$	$\theta(b-y)$	$\theta(B2-V1)$	$\theta(R-I)$	$\theta(V-R)$	$\theta(V-K)$
4308	6.55	0.65	0.408	0.191	0.297	0.396	–	–	–	0.011	0.92	0.911	0.930	–	–	–
5268	6.16	0.92	0.569	0.295	0.403	0.634	0.500	–	–	0.021	1.02	1.075	1.097	1.021	–	–
6254	8.00	0.99	0.607	0.348	0.419	0.671	–	–	–	0.028	1.04	1.110	1.119	–	–	–
6734	6.46	0.85	0.524	0.292	0.351	–	0.470	–	–	0.020	1.00	1.027	–	0.992	–	–
7595	9.72	1.20	–	–	–	–	0.865	–	–	0.030	1.15	–	–	1.377	–	–
10700	3.50	0.72	0.444	0.246	0.250	0.452	0.470	0.62	1.82	0.007	0.96	0.953	0.973	1.001	0.987	0.956
20619	7.05	0.65	0.407	0.206	0.270	0.383	–	–	–	0.027	0.91	0.900	0.912	–	–	–
37828	6.88	1.14	0.727	0.314	0.512	0.849	–	–	–	0.024	1.12	1.214	1.229	–	–	–
71597	7.31	1.16	0.722	0.474	0.468	–	0.60	–	–	0.070	1.08	1.200	–	1.086	–	–
77236	7.51	1.15	0.712	0.437	0.451	0.815	0.62	–	–	0.061	1.10	1.197	1.203	1.112	–	–
107328	4.97	1.16	0.718	0.484	0.521	0.830	0.61	0.89	2.77	0.024	1.08	1.232	1.128	1.129	1.176	–
119971	5.47	1.36	0.847	0.549	0.496	0.989	–	–	–	0.077	1.15	1.328	1.319	–	–	–
130694	4.41	1.38	0.857	0.595	0.459	1.014	0.76	–	–	0.042	1.18	1.366	1.359	1.265	–	–
130952	4.93	0.98	0.606	0.361	0.423	0.662	–	–	–	0.020	1.05	1.115	1.118	–	–	–
136352	5.66	0.65	0.408	0.183	0.292	0.393	0.34	–	–	0.015	0.92	0.908	0.925	0.867	–	–
175329	5.13	1.37	0.838	0.588	0.479	0.995	0.72	–	–	0.055	1.18	1.336	1.336	1.216	–	–
180928	6.07	1.43	0.904	0.581	0.538	1.055	0.83	1.12	3.55	0.056	1.18	1.406	1.381	1.325	1.251	1.346
189567	6.08	0.64	0.407	0.192	0.288	0.391	–	–	–	0.013	0.90	0.908	0.925	–	–	–
203608	4.23	0.49	0.335	0.123	0.309	0.277	0.30	0.47	–	0.006	0.85	0.837	0.847	0.911	–	–
206642	6.29	1.12	0.714	0.385	0.472	0.842	0.62	–	–	0.033	1.10	1.221	1.240	1.132	–	–
208998	7.13	0.57	0.367	0.160	0.321	–	–	–	–	0.021	0.87	0.859	–	–	–	–
211998	5.28	0.65	0.451	0.118	0.236	0.428	–	–	–	0.014	0.97	0.955	0.952	–	–	–
214690	5.87	1.30	0.797	0.597	0.492	0.925	–	–	2.25	0.030	1.09	1.312	1.302	–	–	1.045
219615	3.70	0.92	0.563	0.309	0.425	0.626	0.51	0.72	–	0.013	1.05	1.075	1.096	1.036	1.038	–

Table 3. Atomic lines considered in the region $\lambda\lambda$ 6285-6332 and corresponding excitation potential χ (eV), multiplet number and oscillator strength obtained by fitting the solar spectrum, (a) with a model interpolated in the grids of Bell et al. (1976), (b) with the solar model by Holweger and Müller (1974); $\Delta(\log gf)$ is the difference between (a) and (b), and in column (c) are given gf values given in the references: (1) Blackwell et al. (1982a), (2) Blackwell et al. (1982b), (3) Gurtovenko and Kostik (1981), (4) Lambert (1978), (5) Steffen (1985)

Species	λ (Å)	χ (eV)	Mult.	log gf		$\Delta(\log gf)$	log gf	Ref.
				(a)	(b)		(c)	
VI	6285.165	0.28	19	−2.00	−1.60	−0.40		
Fe I [a]	6286.142	3.08	—	−3.52	−3.41	−0.11		
Fe I	6288.315	3.00	—	−4.24	−4.13	−0.11		
Fe I	6290.532	3.00	208	−4.33	−4.19	−0.14	−4.33	3
Fe I	6290.974	4.73	1258	−0.95	−0.88	−0.07	−0.76	3
VI	6292.816	0.29	19	−1.66	−1.52	−0.14		
Fe I	6293.933	4.83	1260	−1.98	−1.89	−0.09	−1.73	3
VI	6296.495	0.30	19	−1.79	−1.66	−0.13		
Ti I	6296.660	0.00	1	−4.02	−3.94	−0.08		
Fe I	6297.799	2.20	62	−2.97	−2.92	−0.05	−2.74	1, 3
Ti I	6298.084	5.73	144	−2.91	−2.91	0.00		
Fe I [a]	6298.600	3.00	—	−5.29	−5.29	0.00		
Fe I [a]	6299.050	3.00	—	−5.37	−5.37	0.00		
Fe I [a]	6299.414	3.00	—	−4.39	−4.29	−0.10		
Si I	6299.588	3.00	—	−4.20	−4.18	−0.10		
O I	6300.311	0.00	1	−9.77	−9.82	0.03	−9.75	4
Sc II	6300.634	1.51	28	−2.86	−2.85	−0.01	−2.68	5
Sc II	6300.667	1.51	28	−2.27	−2.35	0.08	−2.58	5
Sc II	6300.700	1.51	28	−2.52	−2.55	0.03	−2.79	5
Sc II	6300.719	1.51	28	−2.93	−2.95	0.02	−2.68	5
Fe I	6301.508	3.65	816	−0.72	−0.77	0.05	−0.58	3
Fe I	6301.845	3.64	863	−4.75	−4.67	−0.08		
Fe I	6302.499	3.69	816	−1.29	−1.37	0.08	−1.15	3
Fe I [a]	6302.948	3.00	—	−4.82	−4.82	0.00	−2.66	3
Fe I	6303.461	4.32	1140	−2.96	−2.85	−0.11		
Ti I	6303.767	1.44	104	−1.70	−1.59	−0.11		
Ni I	6305.000	4.27	—	−3.25	−3.25	0.00		
Fe II	6305.314	6.22	200	−2.31	−2.20	−0.11		
Sc I	6305.667	0.02	2	−1.80	−1.62	−0.18		
Sc I	6303.040	0.02	3	−2.62	−2.62	0.00		
Fe I	6306.218	4.59	1230	−4.67	−4.67	0.00		
Fe I	6307.854	3.64	863	−3.65	−3.52	−0.13		
Fe I [a]	6308.813	3.00	—	−4.19	−4.08	−0.11		
Sc II	6309.886	1.50	28	−1.50	−1.50	0.00		
Fe I [a]	6310.266	3.00	—	−3.80	−3.71	−0.09		
Ti I	6311.239	1.44	103	−1.83	−1.66	−0.17		
Fe I	6311.504	2.83	342	−3.42	−3.31	−0.11	−3.21	3
Ti I	6312.241	1.46	104	−1.69	−1.55	−0.14		
Ni I	6314.668	1.93	67	−2.32	−2.32	0.00		
Ni I	6314.668	4.15	249	−2.32	−2.32	0.00		
Fe I	6315.314	4.14	1015	−1.57	−1.56	−0.01		
Fe I	6315.412	4.14	1016	−2.29	−2.21	−0.08		
Fe I	6315.814	4.07	1014	−1.95	−1.87	−0.08	−1.74	3
Fe I	6318.027	2.45	168	−2.19	−2.14	0.04		
Ti I	6318.027	1.43	103	−0.84	−0.84	0.00		
Ca I	6318.610	4.43	53	−1.46	−1.46	0.00		
Mg I	6318.708	5.11	23	−2.15	−2.10	−0.05		
Mg I	6319.242	5.11	23	−2.43	−2.36	−0.07		
Mg I	6319.490	5.11	23	−2.90	−2.85	−0.05		
La II	6320.429	0.17	19	−1.63	−1.63	0.00		
Sc II	6320.843	1.50	28	−2.10	−2.00	−0.10		

Table 3 (continued)

Species	λ (Å)	χ (eV)	Mult.	log gf		Δ (log gf)	log gf	Ref.
				(a)	(b)		(c)	
Ni I	6322.169	4.15	249	−1.36	−1.25	−0.11		
Fe I	6322.694	2.59	207	−2.57	−2.62	0.05	−2.43	2
Ni I	6327.604	1.68	44	−3.23	−3.14	−0.09		
Cr I	6330.096	0.94	6	−3.00	−2.89	−0.11		
Fe I	6330.852	4.73	1254	−1.50	−1.41	−0.09	−1.28	3
Si I	6331.953	5.08	—	−2.67	−2.63	−0.04		
Fe II	6331.953	6.22	199	−2.79	−2.77	−0.02		

[a] Unidentified lines attributed here to Fe I with excitation potential of 3.0 eV

1973). For consistency, the model atmosphere used for the sun is obtained by interpolation in the grids of models by Bell et al. (1976). A solar microturbulence velocity of 1 km s^{-1} was adopted.

The use of the semi-empirical solar model by Holweger and Müller (1974) for obtaining the gf values should provide gf's closer to the absolute values. Table 3 shows the sets of gf's obtained with the use of the two solar models, as well as values from the literature: laboratory measurements by Blackwell et al. (1982a, b) and the values obtained by Gurtovenko and Kostik (1981) where a fitting to the solar spectrum was done, scaling the gf values with basis on the data by Blackwell and collaborators. For the oxygen line the f-value given by Lambert (1978) is indicated.

As a matter of fact, the limitation on the accuracy of abundances is partly set by the accuracy of the gf values used. In the present work this inaccuracy cancels out for the reason that a differential method is employed, which is particularly convenient in the study of stars of solar to moderately deficient metallicities, where all models are interpolated in the same grids of models.

We point out, however, that although the gf's so derived apply conveniently to stellar types relatively close to solar, the observed strong lines with excitation potential χ (eV) > 2.5 appear to be systematically weaker than the computed ones, for the giant stars.

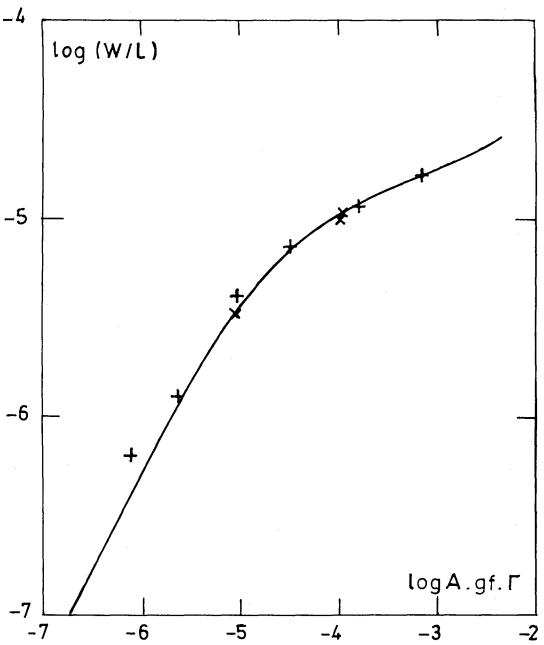

Fig. 1. Curve of growth for one star of the sample: HD 189567. In the ordinates log (equivalent width/wavelength) is represented and in abscissa, log abundance. gf. Γ is given, where Γ is as defined by Cayrel and Jugaku (1963). Symbols: + and × for lines of excitation potential larger and smaller than 3.0 eV respectively

4.2.2. Curves of growth

The metallicity is established with the use of the Fe I curve of growth. The equivalent widths of the lines present in the observed spectra were measured with the IHAP reduction system at ESO, and curves of growth have been built using the code by Spite (1967). Figure 1 shows the curve of growth of Fe I for one star of the sample. In the ordinates the logarithm of equivalent width over wavelength is given as usually, and the abcissa shows the logarithm of the product of the abundance, oscillator strength gf and the factor Γ as defined by Cayrel and Jugaku (1963).

The metallicities derived are in good agreement with data found in the literature, in general.

4.3. The gravity

The determination of the gravity is the major problem: it is obtained essentially by fitting the Sc II line at λ6300.67 Å, for which the hyperfine structure is taken into account, following Steffen (1985). This method is adopted for the reason that the O/Sc ratio should be rather independent of errors, given that the |O I| and Sc II lines form in similar regions of the atmosphere (Lambert et al., 1974; Gratton and Ortolani, 1986). In other words, we impose [Sc/Fe] = 0.0 and then derive [O/Fe]. It seems that, in some cases, the ideal model could be more or less evolved for the star in question; we considered that the O/Sc ratio is relatively parameter-insensitive, and preferred to maintain those parameters.

4.4. Model atmosphere

The atmospheric models used are interpolated in the grids by Bell et al. (1976) and subsequent unpublished models by Gustafsson and collaborators, adopting the same assumptions used to build the original models.

In order to test the stellar parameters, synthetic spectra were computed in the region λλ6285–6333, as described in Barbuy (1988). A further fitting of the stellar atmospheric parameters is

Table 4. Final stellar parameters adopted: reciprocal temperature $\theta_{\rm eff} = 5040/T_{\rm eff}$, gravity log g, metallicity [Fe/H], and microturbulence velocity v_t, measured equivalent widths, derived oxygen-to-iron ratios, and stellar population to which the star probably belongs

HD No.	$\theta_{\rm eff}$	log g	[Fe/H]	v_t (km s^{-1})	W(mÅ) |O I|	[O/Fe]	Error bars	Stellar population
4308	0.91	4.0	−0.4	1.0	3.	−0.10	±0.25	Old disk
5268	1.02	2.7	−0.35	1.5	25.	+0.10	±0.20	Young-old disk
6254	1.07	2.8	−0.25	1.5	26.	+0.15	±0.20	Old disk
6734	0.97	3.2	−0.25	1.0	13.	+0.10	±0.20	Old disk
7595	1.16	1.5	−0.80	1.8	42.	+0.20	+0.2, −0.3	Thick disk
10700	0.98	3.6	−0.60	1.0	5.	+0.05	±0.20	Old disk
20619	0.90	4.0	−0.45	1.0	2.	0.0	±0.25	Old disk
37828	1.18	1.6	−1.20	1.8	42.	+0.32	+0.2, −0.3	Halo
71597	1.18	1.9	−0.40	1.8	31.	+0.05	+0.2, −0.3	Thick disk
77236	1.18	1.7	−0.70	1.8	42.	+0.18	+0.2, −0.3	Halo-thick disk
107328	1.17	2.3	−0.20	1.7	61.	+0.15	+0.2, −0.3	Young disk
119971	1.25	1.1	−0.80	1.8	64.	+0.27	+0.2, −0.3	Old disk
130694	1.26	1.0	−0.75	2.0	75.	+0.20	+0.2, −0.3	Old disk
130952	1.08	2.3	−0.25	1.5	26.	+0.10	±0.20	Old disk
136352	0.90	3.8	−0.40	1.0	5.	+0.10	±0.20	Thick-old disk
175329	1.18	1.7	−0.55	1.8	70.	+0.30	+0.2, −0.3	Halo
180928	1.26	1.2	−0.55	1.8	66.	+0.13	+0.2, −0.3	Halo-old disk
189567	0.90	4.1	−0.30	1.0	6.	+0.05	±0.20	Old-young disk
203608	0.86	4.0	−0.80	1.6	3.	+0.15	±0.25	Old disk
206642	1.14	2.0	−0.75	1.8	35.	+0.25	+0.2, −0.3	Thick disk
208998	0.87	3.6	−0.40	1.0	5.	0.0	±0.20	Thick-old disk
211998	0.96	3.4	−1.60	1.0	7.	+0.40	±0.20	Halo
214690	1.24	1.9	−0.10	1.8	65.	+0.10	+0.2, −0.3	Old disk
219615	1.05	2.3	−0.50	1.5	32.	+0.15	±0.20	Old disk

done: the ionisation and excitation equilibria are tested by checking the intensity of the individual lines.

The final model parameters adopted are shown in Table 4.

4.5. *The molecular dissociative equilibrium*

The molecular dissociative equilibrium is computed at each level of the model atmosphere, following Tsuji (1973), with the inclusion of 18 elements and 35 molecules. The following oxygen compounded molecules are considered: MgO, TiO, H_2O, CO, NO, OH, O_2, SiO, CaO, ScO, FeO, CuO. The CO molecule is responsible for the major oxygen consumption at the expense of free oxygen atoms at low temperatures ($\theta > 1.12$); the use of the correct carbon abundance for the cool stars is therefore recommended.

Carbon and nitrogen abundances are available in the literature for some stars of the present sample. The results by Laird (1985) were used to establish values consistent with our stellar parameters, for the following stars: ([C/Fe], [N/Fe]) = (0.15, 0.35) for HD 4308, (0.33, −0.17) for HD 10700, (−0.15, 0.20) for HD 203608, (0.15, −0.35) for HD 211998. For the remaining stars [C/Fe] = [N/Fe] = 0.0 was adopted.

4.6. *Errors*

The main source of uncertainty in the oxygen abundances are the stellar parameters. The following reasoning can be followed regarding the temperature, gravity and metallicity, determined as described above: the metallicity can be supposed to be correct within ±0.1 dex, if the temperature and the oscillator strengths gf's are correct. The accuracy of the gf's obtained by fitting the solar spectrum is discussed by Rutten (1988). In our case, given that we work differentially with respect to the sun, the absolute values of gf are not required in fact, but rather they have to be consistent within the grid of models used. Therefore we consider to have an uncertainty of 0.1 dex in the metallicities.

The temperature can be supposed to be correct within ±200 K. With basis on the derivation of the temperatures from the photometric indices (Table 2), the final temperature adopted has to satisfy the excitation equilibrium, i.e., lines of different excitation potential have to show the same abundance. This latter point is again related to the accuracy of the oscillator strengths. It was considered that the medium intensity to weak lines are more reliable than the strong lines.

Errors coming from the molecular dissociative equilibrium are mainly due to the carbon abundance introduced in the calculations. The influence of molecular formation is negligible for stars hotter than $\theta < 1.12$. For the cooler stars, the CO formation affects the intensity of the oxygen lines. If [C/Fe] < 0 in the real star but [C/Fe] = 0 is adopted, the oxygen abundance is overestimated, but by not more than 0.1 dex for the temperatures considered here (see Barbuy, 1988). Given that the cooler stars are also evolved, showing gravities log $g < 2.3$, where mixing effects are expected to lower the carbon abundance, it can be considered that an error of −0.1 dex in the oxygen abundance is introduced.

Finally, for faint oxygen lines, the oxygen abundance derived is slightly less precise.

The error bars given in Table 4 and in Fig. 4a take into account the factors discussed in this section.

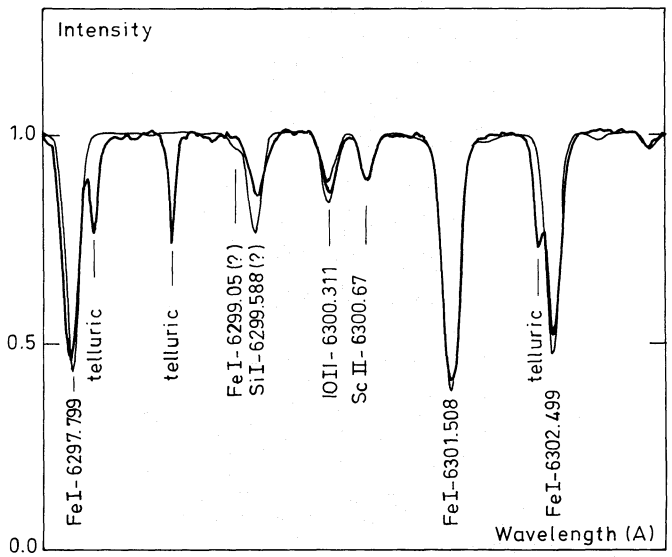

a

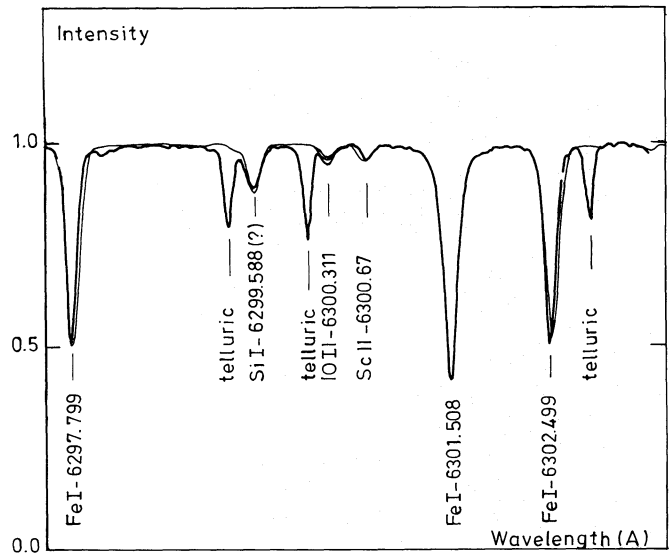

b

Fig. 2a and b. Observed Reticon spectrum (thick line) and synthetic spectra (thin lines) at $\lambda\lambda$6297–6303, for **a** HD 5268, where [O/Fe] = 0.0, +0.1 and +0.2, **b** HD 10700, where [O/Fe] = −0.05, +0.05, and +0.15

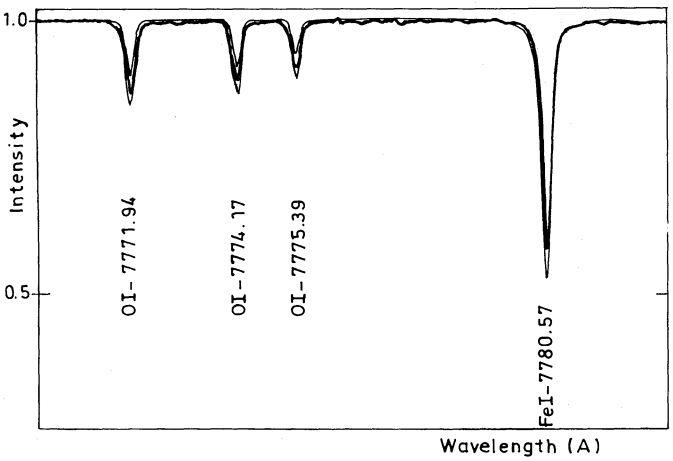

Fig. 3. The oxygen triplet at $\lambda\lambda$7771–7775, for the star HD 10700. The thick line is the observed Reticon spectrum and the thin lines are the synthetic spectra computed with [O/Fe] = 0.0, +0.2, and +0.4

5. The oxygen abundances

5.1. Results

The oxygen abundances were obtained by computing synthetic spectra to fit the |O I| λ6300.311 line. The calculations assume local thermodynamic equilibrium (LTE) and the molecular dissociative equilibrium is taken into account; more details are given in Sect. 4 and in Barbuy (1988). In Table 4 are given the stellar parameters adopted, the equivalent width of the |O I| λ6300 line, the resulting oxygen-to-iron ratios and corresponding error bars, and the probable population to which each star belongs. Figure 2 illustrates the method.

Figure 4 gives the behaviour of oxygen-to-iron with respect to the stellar metallicity. In Fig. 4a the error bars are indicated. In this figure is also shown the behaviour of oxygen-to-iron versus iron-to-hydrogen as predicted by Matteucci and Greggio (1986), corresponding to a line [O/Fe] = −0.56 [Fe/H]. The present data suggest a different slope: [O/Fe] = −0.23 [Fe/H] in the disk. In Fig. 4b are also plotted the results obtained by Barbuy (1988) for halo stars.

The present results seem to show that the mean value of the oxygen-to-iron ratio at metallicities [Fe/H] > −0.5 is lower than in the transition phase −0.8 < [Fe/H] < −0.5.

The same effect seems to be present in the results by Kjaergaard et al. (1982) and Gratton and Ortolani (1986), whereas in the results by Clegg et al. (1981) and Nissen et al. (1985) the oxygen-to-iron ratio decreases monotonically reaching the solar value at solar metallicities. In agreement with these latter authors, a gradual increase of the oxygen-to-iron ratio for decreasing metallicities, with a starting point at [Fe/H] = 0.0 is predicted in the models of disk metal enrichment by Twarog and Wheeler (1982) and Matteucci and Greggio (1986). On the other hand, the yields in a two-zone model might differ from these.

A comparison of the results by the different authors is shown in Fig. 5, for the metallicity range −1.0 < [Fe/H] < +0.5.

It seems clear that oxygen is overabundant relative to iron at [Fe/H] = −0.8, but at the low metallicity end, it is not clear at which metallicity the oxygen-to-iron ratio starts to drop. This is partly due to the fact that only a low number of stars in this metallicity range are easily observable.

In order to establish the behaviour of the oxygen-to-iron ratio in the ranges −1.2 < [Fe/H] < −0.8 and −0.6 < [Fe/H] < 0.0, homogeneous determinations for a far greater sample of stars, including all populations, is necessary.

5.2. The $\lambda\lambda$7771–7775 triplet lines

For the subgiant HD 10700, the O I triplet at λ7771.94, λ7774.17 and λ7775.39 was also observed, using the Reticon as detector.

The oscillator strengths are adopted from Lambert (1978): $\log gf = 0.33$, 0.19 and −0.03 respectively.

Figure 3 shows the observed and synthetic spectra for HD 10700 computed with [O/Fe] = 0.0, 0.2, and 0.4, where the good fit of the O I lines is found for [O/Fe] = +0.20, therefore 0.15 dex higher than the result obtained with the |O I| λ6300 line.

This difference could be systematic and therefore explain the difference between oxygen-to-iron ratios found, on the one hand

Table 5. Kinematical and chemical properties of the different populations in the Galaxy. U, V, W are the velocities in galactic coordinates, $\sigma(U, V, W)$ are the dispersions in these velocities; e is eccentricity, [Fe/H] is the mean metallicity spanning over the intervals indicated in parentheses, and the last column indicates the rotation lag behind the local standard of rest (LSR)

Population	Scale height (pc)	V (km s^{-1})	W (km s^{-1})	$\sigma(U):\sigma(V):\sigma(W)$ (km s^{-1})	e	$\overline{[Fe/H]}$	Rotation lag behind LSR (km s^{-1})
Young thin disk	100					0.0 (0.15)	0
Old thin disk	300–350	− 40		35 : 25 : 20		−0.3 (0.2)	20
Thick disk	>1000	>100	<60	80 : 60 : 45	$0.4<e<0.45$	−0.6 (0.3)	50
Spheroid	4000	<100	>60	150 : 120 : 120	>0.59	−1.5 (0.5)	220

by Clegg et al. (1981) and Nissen et al. (1985), who used the triplets at λ7770 and λ9265, and on the other hand, the results of the present work, as well as those by Kjaergaard et al. (1982) and Gratton and Ortolani (1986), based on the |O I| λ6300 line.

There seems to be a systematic difference Δ [O/Fe] > 0 in the sense triplet minus forbidden lines. It is known that the triplet lines are subject to non-LTE effects, and that the discrepancy between a LTE and a non-LTE computed line increases with the strength of the line; however, it remains to be verified whether this could account for the differences in the oxygen-to-iron ratios.

5.3. *Sulphur and oxygen*

It must be pointed out that the results for sulphur by Clegg et al. (1981) and François (1987, 1988) show a sulphur-to-iron ratio above solar for all metallicities below solar. Sulphur and oxygen are "twin" elements from the nucleosynthesis point of view, and their enrichment in the Galaxy should follow the same scheme of chemical evolution, although some enrichment in S by carbon deflagration supernovae is expected (Thielemann et al., 1986).

6. Stellar populations and the oxygen abundance

6.1. *Stellar populations*

The existence of at least two different stellar populations in the Galaxy, the disk and the halo stars, is widely accepted. Observational evidences seem to exist for a third component, the thick disk stars, but this still is a contentious issue.

Lindblad (1925) has been the first author to suggest an "intermediate kinematic component" for our Galaxy. The so-called "thick disk" was suggested by observations of edge-on S0 galaxies by Burnstein (1979). This component becomes more and more diluted as one goes to the later type spirals. An extension of the denomination "thick disk" for our Galaxy was introduced by Gilmore and Reid (1983), based on the density distribution of stars versus distance from the galactic plane for large samples of stars, at different directions.

From observational studies of different stellar samples, the characteristics given in Table 5 can be adopted for the stellar populations of the Galaxy, as given in Freeman (1986), Gilmore and Reid (1983), Gilmore and Wyse (1986), Mihalas and Binney (1981), Norris (1986), Sandage (1986), Sandage and Fouts (1987), and Wyse and Gilmore (1986).

In Table 4, the stars of the present sample are tentatively classified in one of the 3 populations, with basis on their kinematical plus chemical characteristics given in Tables 1 and 4. Most of them belong to the old thin disk. One "certain" thick disk star is HD 7595. As a matter of fact, this star is presented by Norris (1986) as a candidate for the thick disk population, with the constraints: distance $z \geqq 600$ pc, $-0.88 < [Fe/H] < -0.6$ (although Norris, 1987 drops his earlier suggestion of a thick disk, supposing that there is rather a continuous transition between the thin disk and the halo).

6.2. *Oxygen abundances and chemical evolution*

Oxygen is produced at the helium burning phase in massive stars, being thus rapidly ejected to the interstellar medium.

The results by Barbuy (1988) suggest that the first stars have produced oxygen and iron in the same relative amounts, [O/Fe] being a constant at all halo metallicities ($-3.0 < [Fe/H] < -1.3$).

The subsequent enrichment in iron, produced then by intermediate mass stars, brings the oxygen-to-iron ratio to lower values. The transition point at the end of the halo phase, from which point the oxygen-to-iron ratio starts to decrease due to the iron enrichment by the intermediate-mass stars is not very well defined.

From the data of Figs. 4 and 5, we can see that:

a) It seems well established that oxygen is obserabundant relative to iron for metallicities around [Fe/H] = −0.8. We remind that this is the metallicity typical of the thick disk (see Table 5).

b) For the higher metallicities, it is not clear if the scatter in [O/Fe] in the range $-0.8 < [Fe/H] < -0.5$ is cosmic or is due to the errors in the determinations. The two-zone models (Jones and Wyse, 1983; Gilmore and Wyse, 1986) would predict an average residual metallicity of the gas from the halo around −1.4 dex, at the formation of the thick disk, and an average metallicity at the transition between thick and thin disk around −0.6 dex. Therefore it could be that the oxygen-to-iron ratio presents transition values at these two metallicities as well.

c) The value of [O/Fe] in the range $-1.3 < [Fe/H] < -0.8$ is not well established. The few determinations available, as presented in Fig. 2 of Sneden (1985), show the halo oxygen abundance. In order to confirm this result, the study of a larger number of stars in this range is necessary. This could be somewhat difficult if the particularly illustrative plot of the ultraviolet excess versus [Fe/H] by Carney (1979), where a gap exists in the number of stars in that range, is considered.

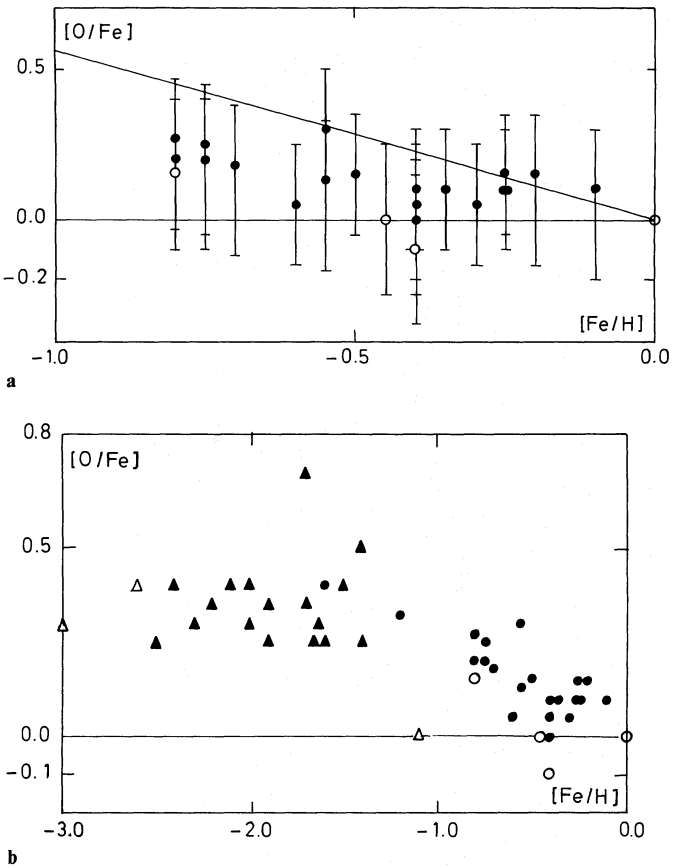

Fig. 4a and b. [O/Fe] versus [Fe/H]. **a** Present results for the range $-1.0 < [Fe/H] < 0.0$, where error bars are shown. The line drawn corresponds to predictions by Matteucci and Greggio (1986). **b** Present results and those of Barbuy (1988), given in the range $-3.0 < [Fe/H] < 0.0$. Symbols: ● and ○: present work; ▲ and △: Barbuy (1988), where ○, △ represent uncertain results due to the weakness of the |O I| line. ⊙ represents the solar value

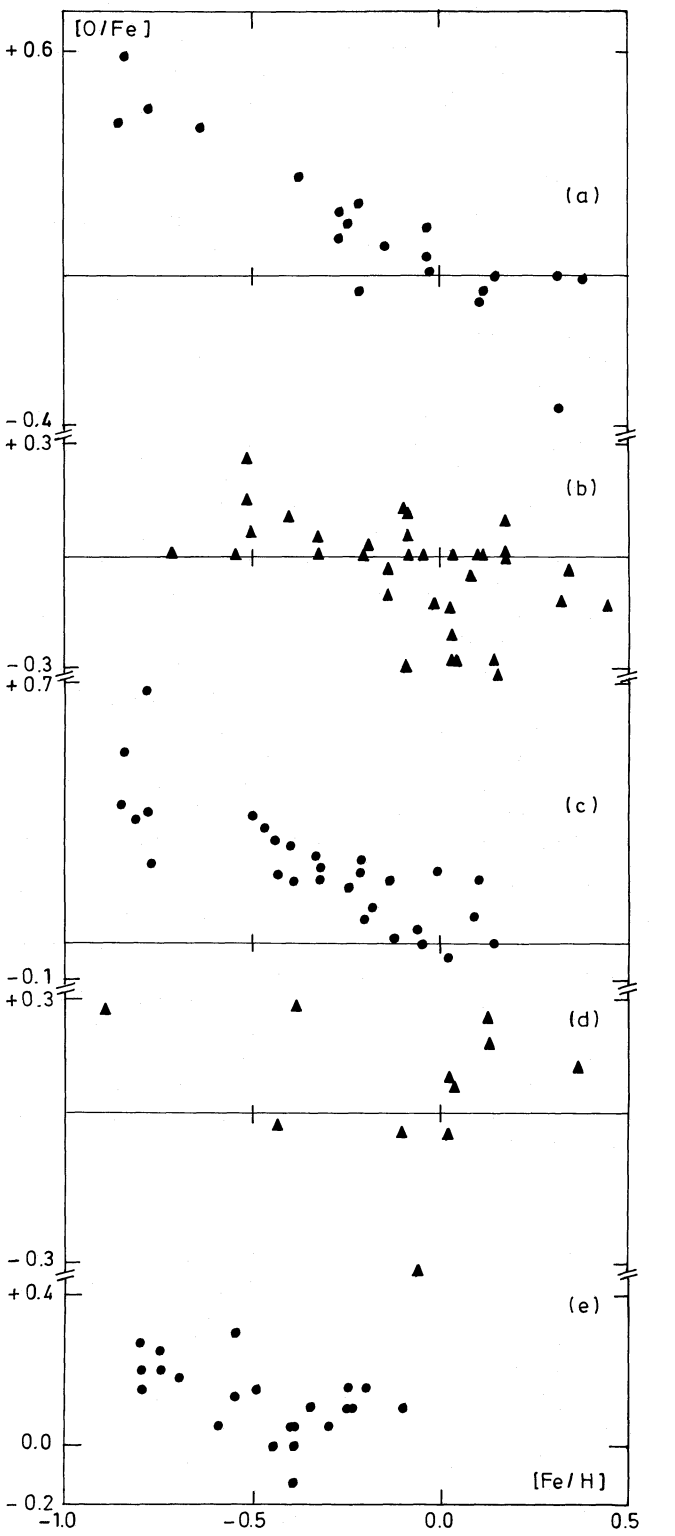

Fig. 5a–e. [O/Fe] versus [Fe/H] in the metallicity region $-1.0 < [Fe/H] < +0.5$ by different authors, disposed in the chronological order: **a** Clegg et al. (1981), **b** Kjaergaard et al. (1982), **c** Nissen et al. (1985), **d** Gratton and Ortolani (1986), **e** present work

6.3. A crude scenario

The constancy of the oxygen-to-iron ratio in the halo suggests that the massive stars of different masses produce oxygen and iron in roughly constant proportions. Time scales of stellar evolution and of the early stages of the Galaxy lifetime impose that the halo stars formed from a gas enriched only by the first generation massive stars.

Along the galaxy collapse, this gas falls into the volume of the so-called thick disk; at the time of formation of the thick disk, halo intermediate mass stars enrich the gas in iron. An intermediate population forms in this volume, which will itself cause an enrichment again by the most massives stars of this thick disk population.

At this phase it is expected that stars forming in different regions of space will show [O/Fe] higher than in the halo, if it is formed in the vicinity of a type II supernova, or lower than in the halo, if the region is contaminated by the Fe-enriched matter coming from the halo intermediate mass stars. If the initial gas in the thick disk has $[Fe/H] = -1.4$, their stars should show metallicities spanning from $-1.4 < [Fe/H] < -0.6$ (limits given by Gilmore and Wyse, 1986) and oxygen-to-iron ratios $0.0 < [O/Fe] < +0.8$; in Fig. 5 it can be seen that $0.2 < [O/Fe] < 0.7$ at $[Fe/H] = -0.8$.

Later on, the thin disk has a history in the same lines as the thick disk, but showing metallicities in the range $-0.6 < [Fe/H] < +0.2$ (the upper limit is controversial) and showing a mean oxygen-to-iron ratio closer to the solar value.

7. Conclusion

The oxygen-to-iron ratio was derived for 24 moderately metal-poor stars, most of them belonging to the old thin disk and some to the thick disk population.

From the results obtained, the following remarks and conclusions can be made:

(1) Oxygen seems to be overabundant relative to iron at $[Fe/H] = -0.8$.

(2) At the metallicities $-1.3 < [Fe/H] < -0.8$, only a few oxygen abundance determinations are available in the literature: Fig. 2 by Sneden (1985) shows that the oxygen-to-iron ratio has the halo value in this range, and that the point where it stars to drop toward the solar value would be around $[Fe/H] = -0.8$. More work in this metallicity region would be of interest.

(3) In the metallicity range $-0.8 < [Fe/H] < -0.5$, corresponding to the thick disk, the oxygen-to-iron ratios show a scatter, which is however within the error base. It can be attributed to the errors involved in the determinations; otherwise, if future data indicate a cosmic scatter, this would be a confirmation of the thick-disk phase during the evolution of the Galaxy.

(4) A discrepancy seems to exist between oxygen abundances derived from the O I permitted triplet lines at $\lambda 7770$ and $\lambda 9265$, and the forbidden lines at $\lambda 6300$ (and $\lambda 6363$). An investigation on the non-LTE effects on the triplet lines would be of great interest.

Acknowledgements. We are grateful to A. Gomez, M. Grenon, M. Spite, and F. Spite for enriching discussions, and to H. Lindgren and A. Ardeberg for providing data in advance of publication. We are also grateful to the referee P.E. Nissen for very helpful comments on an earlier version of this paper. The computations were done at the Burroughs 6900 of the Universidata de Sao Paulo and at the VAX 8600 of the Observatoire de Paris-Meudon. This research was partially supported by the FAPESP (Sao Paulo). M.E.M is supported by FAPESP, fellowship no. 85/3644-4.

References

Barbuy, B.: 1985a, *Astron. Astrophys.* **151**, 189
Barbuy, B.: 1985b, in *Production and Distribution of C, N, O elements*, ESO workshop and proceedings no. 21, eds. I.J. Danziger, F. Matteucci, K. Kjaer, p. 49
Barbuy, B.: 1988, *Astron. Astrophys.* **191**, 121
Bell, R.A., Eriksson, K., Gustafsson, B., Nordlund, A.: 1976, *Astron. Astrophys. Suppl.* **23**, 37
Blackwell, D.E., Petford, A.D., Shallis, M.J., Simmons, G.J.: 1982a, *Monthly Notices Roy. Astron. Soc.* **199**, 43
Blackwell, D.E., Petford, A.D., Simmons, G.J.: 1982b, *Monthly Notices Roy. Astron. Soc.* **201**, 595
Bond, H.E.: 1980, *Astrophys. J. Suppl.* **44**, 517
Burnstein, D.: 1979, *Astrophys. J.* **234**, 829
Carbon, D.F., Barbuy, B., Kraft, R.P., Friel, E., Suntzeff, N.B.: 1987, *Pub. Astron. Soc. Pacific* **99**, 335
Carney, B.W.: 1979, *Astrophys. J.* **233**, 211
Carney, B.W.: 1980, *A Catalogue of Field Population II Stars*, Washington
Carney, B.W.: 1983, *Astron. J.* **88**, 623
Cayrel, R., Jugaku, J.: 1963, *Ann. Astrophys.* **26**, 495
Clegg, R.E.S., Lambert, D.L., Tomkin, J.: 1981, *Astrophys. J.* **250**, 262
Delbouille, L., Roland, G., Neven, L.: 1973, *Photometric Atlas of the Solar Spectrum from 3000 to 10000 A*, Institut d'Astrophysique de Liège
Eggen, O.J.: 1966, Roy. Obs. Bull. no. 120
Eggen, O.J.: 1979, *Astrophys. J.* **229**, 158
Eggen, O.J., Lynden-Bell, D., Sandage, A.: 1962, *Astrophys. J.* **136**, 748
François, P.: 1987, *Astron. Astrophys.* **176**, 294
François, P.: 1988, *Astron. Astrophys.* **195**, 226
Freeman, K.C.: 1986, in *Stellar Populations*, eds. C.A. Norman, A. Renzini, M. Tosi, Cambridge University Press, p. 227
Gilmore, G., Reid, I.N.: 1983, *Monthly Notices Roy. Astron. Soc.* **202**, 1025
Gilmore, G., Wyse, R.F.G.: 1985, *Astron. J.* **90**, 2015
Gilmore, G., Wyse, R.F.G.: 1986, *Nature* **322**, 806
Golay, M.: 1980, *Vistas in Astronomy* **24**, 141
Gratton, R.G., Ortolani, S.: 1986, *Astron. Astrophys.* **169**, 201
Gurtovenko, E.A., Kostik, R.I.: 1981, *Astron. Astrophys. Suppl.* **46**, 239
Hansen, L., Kjaergaard, P.: 1971, *Astron. Astrophys.* **15**, 123
Holweger, H., Muller, E.A.: 1974, *Solar Phys.* **39**, 19
Jones, B.J.T., Wyse, R.F.G.: 1983, *Astron. Astrophys.* **120**, 165
Kjaergaard, P., Gustafsson, B., Walker, G.A.H., Hultqvist, L.: 1982, *Astron. Astrophys.* **115**, 145
Laird, J.B.: 1985, *Astrophys. J.* **289**, 556
Lambert, D.L.: 1978, *Monthly Notices Roy. Astron. Soc.* **182**, 249
Lambert, D.L., Sneden, C., Ries, L.M.: 1974, *Astrophys. J.* **188**, 97
Lindblad, B.: 1925, *Ark. F. Mat. Astr. och Fysik* **19A**, no. 21
Matteucci, F., Greggio, L.: 1986, *Astron. Astrophys.* **154**, 279
Mihalas, D., Binney, J.: 1981, *Galactic Astronomy: Structure and Kinematics*, Freeman, San Francisco
Nissen, P.E., Edvardsson, B., Gustafsson, B.: 1985, in *Production and Distribution of C, N, O elements*, ESO workshop and proceedings no. 21, eds. I.J. Danziger, F. Matteucci, K. Kjaer, p. 131
Norris, J.: 1986, *Astrophys. J. Suppl.* **61**, 667
Norris, J.: 1987, *Astrophys. J.* **314**, L39
Norris, J., Bessell, M.S., Pickles, A.: 1985, *Astrophys. J. Suppl.* **58**, 463
Rufener, F.: 1981, *Astron. Astrophys. Suppl.* **45**, 207
Rutten, R.J.: 1988, in *The Impact of Very High S/N Spectroscopy on Stellar Physics*, *IAU Symp.* **132**, eds. G. Cayrel de Strobel, M. Spite, p. 367
Sandage, A.: 1970, *Astrophys. J.* **162**, 841
Sandage, A.: 1986, in *Stellar Populations*, eds. C.A. Norman, A. Renzini, M. Tosi, Cambridge University Press, p. 29
Sandage, A., Fouts, G.: 1987, *Astron. J.* **92**, 74
Sneden, C.: 1985, in *Production and Distribution of C, N, O elements*, ESO workshop and proceedings no. 21, eds. I.J. Danziger, F. Matteucci, K. Kjaer, p. 1
Spite, M.: 1967, *Ann. Astrophys.* **30**, 211
Steffen, M.: 1985, *Astron. Astrophys. Suppl.* **59**, 403
Stone, R.P.S.: 1983, *Publ. Astron. Soc. Pacific* **85**, 27
Thielemann, F.K., Nomoto, K., Yokoi, K.: 1986, *Astron. Astrophys.* **158**, 17
Tsuji, T.: 1973, *Astron. Astrophys.* **23**, 411
Twarog, B.A., Wheeler, J.C.: 1982, *Astrophys. J.* **261**, 636
VandenBerg, D.A., Bell, R.A.: 1985, *Astrophys. J. Suppl.* **58**, 561
Wyse, R.F.G., Gilmore, G.: 1986, *Astron. J.* **91**, 855